JOURNAL OF SOLID STATE CHEMISTRY 101, 173–185 (1992)

Nature of Hole States in Cuprate Superconductors

APURVA MEHTA, JOSEPH DiCARLO,
AND ALEXANDRA NAVROTSKY

Princeton Materials Institute and Department of Geological and Geophysical Sciences, Princeton University, Princeton, New Jersey 08544

Received February 27, 1992; in revised form April 27, 1992; accepted April 29, 1992

This study addresses the nature of the hole states in the high oxidation state cuprates. From the thermochemistry of oxidation in the cuprate superconductors, specifically in $La_{2-x}A_xCuO_{4-x/2+\delta}$ (A = Ba, Sr, Ca, Pb) and $YBa_2Cu_3O_{6-\delta}$, a model is proposed that assigns a major fraction of the holes in these "Cu^{3+}" materials to states which chemically are "peroxidelike," involving holes paired on adjacent oxygens. Based on this hypothesis previously reported structural observations on $NaCuO_2$, $KCuO_2$, $La_{2-x}Sr_xCuO_{4-x/2+\delta}$, and $YBa_2Cu_3O_{6+\delta}$ are modeled. Electrical properties (including superconductivity) of the high oxidation state cuprates are closely related to these structural trends.

Introduction

Ever since the discovery of superconductivity in the La,A,Cu,O (A = Ba, Sr, Ca) systems, there has been a surge of interest in high oxidation state cuprates. Presently, it is believed that the highest superconducting transitions are found in materials in which all of the acceptors are compensated by mobile holes. However, there is considerable disagreement on whether the holes in these systems are on Cu^{2+}, creating Cu^{3+} species (*1*, *2*), on O^{2-}, forming O species (*3*, *4*, *51*), or whether significant covalency renders this distinction moot. The proper description of the location and the nature of holes is of primary importance in the formulation of a theory of superconductivity.

In this paper, we propose a *chemical* description for the holes in the high oxidation cuprates. This description links the thermochemical systematics and bond lengths to the properties of a well-known chemical species, the peroxide ion O_2^{2-}. The proposed "peroxidelike" hole pairs offer a simple model consistent with these chemical observables. This model does not attempt to describe the physics of the hole states but highlights the chemical similarity of those states in a variety of high oxidation cuprates, some of which are superconducting but others not even conducting. A direct correlation between the peroxidelike pair concentration of T_c suggests that there may be some *physical* significance to the peroxidelike hole states. However, the detailed physical implications of this model are beyond the scope of this paper.

Thermochemical Observations

At high temperature acceptor doped lanthanum cuprate, $La_{2-x}A_xCuO_{4-x/2+\delta}$ (A = Ba, Sr, Ca, and Pb), is oxygen deficient.

0022-4596/92 $5.00

Here, δ denotes the oxygen in excess of the stoichiometric composition (the n = p point). In other words, δ is half the number of (excess) holes in the material. The oxygen deficiency ($x/2 - \delta$) is accommodated as oxygen vacancies (*4–7*). Neutron diffraction analyses of Kamiyama *et al.* (*5*), Jorgensen *et al.* (*8*), and Cava *et al.* (*9*) indicate that the oxygen vacancies in $La_{2-x}A_xCuO_{4-x/2+\delta}$ are located at the basal oxygen sites preferentially over the apical ones.

At lower temperature and higher oxygen fugacity $La_{2-x}A_xCuO_{4-x/2}$ oxidizes. The excess oxygen, δ, can enter the $La_{2-x}A_xCuO_{4-x/2+\delta}$ structure by either occupying an interstitial site or filling an oxygen vacancy. The oxygen vacancies are coupled to the interstitial oxygen defects via the Frenkel reaction [in the Kroger–Vink defect notation (*10*)].

$$O_O + V_I = O_I'' + V_O^{\cdot\cdot} \qquad (1)$$

The two modes of oxygen incorporation, creation of oxygen interstitials and occupation of oxygen vacancies, are not independent of each other. Under certain circumstances, however, the process of oxygen incorporation can almost entirely be accounted for by only one of the processes. For example, in a sample with a large vacancy concentration it would be impossible for a significant amount of the oxygen incorporation to occur via interstitial formation. Since $La_{2-x}Sr_xCuO_{4-x/2}$ has a large number of oxygen vacancies the defect chemical reaction for the oxidation can be simplified to

$$V_O^{\cdot\cdot} + \tfrac{1}{2}O_2 \rightarrow O_O + 2\,h^{\cdot}, \qquad (2)$$

where $V_O^{\cdot\cdot}$ are the basal plane vacancies generated on acceptor (A) incorporation at high temperatures and $h^{\cdot}$ are holes, responsible for charge transport in the material (*11*).

The oxygen excess, δ, in $La_{2-x}A_xCuO_{4-x/2+\delta}$ is a function of temperature, pressure, oxygen fugacity, and the acceptor content of the material. It has been shown that there is thermochemical continuity over the entire range of acceptor doping in these materials (*12*, *13*); i.e., the measured enthalpies appear to fall on a single smooth curve as a function of composition. The enthalpy of oxidation of $La_{2-x}A_xCuO_{4-x/2+\delta}$ has been determined at fixed x by high temperature reaction calorimetry (*12*, *13*). Similar studies were performed earlier on $YBa_2Cu_3O_X$ (*14*), which behaves as a highly acceptor-doped material (*15*, *16*) and can be viewed as Ba-doped, perovskitelike $YCuO_x$ (*17*). The enthalpies of oxidation of $La_{2-x}Sr_xCuO_{4-x/2+\delta}$ (for x = 0.30, 0.75, and 1.00), $La_{2-x}Ba_xCuO_{4-x/2+\delta}$ (x = 0.30), and $YBa_2Cu_3O_{6+\delta}$ are shown in Table I. The enthalpies of oxidation for the Sr-doped La_2CuO_4 are independent of the Sr content within the uncertainty of the measurements. However, the enthalpy of oxidation of the Ba-doped La_2CuO_4 is significantly more exothermic than that for the Sr doped series, but is similar to the enthalpy of oxidation of

TABLE I

ENTHALPY OF OXIDATION OF CUPRATE SUPERCONDUCTORS AND ALKALINE EARTH OXIDES

$$La_{2-x}A_xCuO_{4-x/2+\delta} + \frac{(\delta' - \delta)}{2}O_2 \rightarrow La_{2-x}A_xCuO_{4-x/2+\delta'}$$

A_x	Enthalpy (kJ/mole of O)
$Sr_{0.3}$	-60 ± 25^a
$Sr_{0.75}$	-65 ± 10^b
$Sr_{1.00}$	-65 ± 10^b
$Ba_{0.3}$	-110 ± 25^c

$$YBa_2Cu_3O_{6+\delta} + \frac{\delta' - \delta}{2}O_2 \rightarrow YBa_2Cu_3O_{6+\delta'}$$

Enthalpy (kJ/mole of O)
-95 ± 4^d

$$AO + \tfrac{1}{2}O_2 \rightarrow AO_2$$

A	Enthalpy (kJ/mole of O)
Sr	-55 ± 20^e
Ba	-85 ± 30^e

[a] Uncertainties are reported as two times the standard deviation of the mean.
[b] Value is taken from (*12*).
[c] Value is taken from (*13*).
[d] Value is taken from (*14*).
[e] Value is taken from (*24*).

$YBa_2Cu_3O_X$ [where it is constant across the entire composition range, $0 < X < 1$ (*14*)]. The energetic ease of oxidation in these materials, thus, appears to be determined primarily by the nature of the divalent dopant cation and seems to be independent of the amount of acceptor doping or the electronic state (superconducting, metallic, or semiconducting) of the material. These observations also support the qualitative chemical concept the large "basic" cations stabilize transition metals in high oxidation states in perovskitelike structures. Less complete thermochemical data for Pb- and Ca-doped La_2CuO_4 also support these trends (*13*).

The enthalpy of formation of $La_{2-x}A_xCuO_{4-x/2}$ (A = Ba, Sr, Ca, and Pb) from component oxides, represented by the following equation,

$$\left(1-\frac{x}{2}\right)La_2O_3 + xAO + CuO \rightarrow La_{2-x}A_xCuO_{4-x/2}, \quad (3)$$

is shown in Fig. 1a as a function of the acceptor concentration. The reaction represents the formation of a compound with no extrinsic holes (or electrons)—a "fully reduced" compound. The acceptors in the fully reduced compound are completely compensated by oxygen vacancies. On oxidation of such a compound the oxygen vacancies are filled, with the generation of extrinsic holes, which charge compensate the acceptors. The material with a fully occupied oxygen (and cation) lattice (henceforth referred to as the "fully oxidized" compound) from component oxides can be represented as follows:

$$\left(1-\frac{x}{2}\right)La_2O_3 + xAO + \frac{x}{4}O_2 + CuO \rightarrow La_{2-x}A_xCuO_4. \quad (4)$$

The difference between the enthalpy of Reactions (3) and (4) is the enthalpy of oxidation of $La_{2-x}A_xCuO_{4-x/2+\delta}$, with an enthalpy of -65 kJ/mole of O for Sr-doped

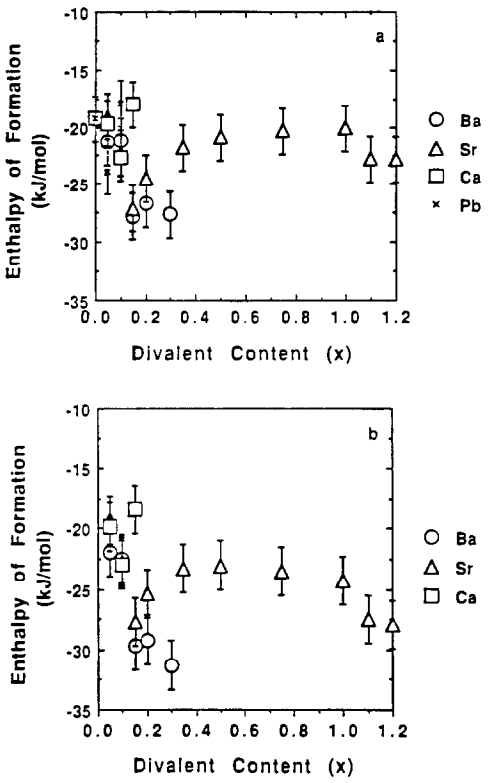

FIG. 1. (a) Enthalpy of formation of $La_{2-x}A_xCuO_{4-x/2}$ (A = Ba, Sr, Ca, Pb) from the component oxides. (b) Enthalpy of formation of the "fully oxidized" $La_{2-x}A_xCuO_4$ (A = Ba, Sr, Ca) from the component peroxides and oxides. Refer to the text for details.

materials and enthalpy of -110 kJ/mole of O for Ba-doped materials (see Table I). The formation of fully oxidized a-doped lanthanum cuprate can also be represented as

$$\left(1-\frac{x}{2}\right)La_2O_3 + \frac{x}{2}AO + \frac{x}{2}AO_2 + CuO \rightarrow La_{2-x}A_xCuO_4. \quad (5)$$

Reaction (5) represents a formation cycle that is free of gaseous species. Figure 1b shows the enthalpy of formation of $La_{2-x}A_xCuO_4$ from the component oxides and peroxides [Eq. (5)] as a function of the acceptor concentration. Figures 1a and 1b look similar; thus, the enthalpy of reaction (5) is simi-

lar to the enthalpy of Reaction (3) for a given x. From Reaction (3–5) and the similarity between Figs. 1a and 1b, it can be deduced that the enthalpy of oxidation of $La_{2-x}A_xCuO_{4-x/2+\delta}$ is very similar to the enthalpy of oxidation of the corresponding alkaline oxide (AO) to the alkaline peroxide, given by the following reaction:

$$AO + \tfrac{1}{2}O_2 \rightarrow AO_2. \qquad (6)$$

This is indeed the case (see Table I).

In $La_{2-x}A_xCuO_{4-x/2+\delta}$, oxygen ions fill basal vacancies [see Reaction (2)] which are presumably in the vicinity of the alkaline earth acceptors to maintain local electroneutrality of the lattice. The separation of the alkaline earth cation and the entrant oxygen is similar in $La_{2-x}A_xCuO_{4-x/2+\delta}$ [2.73 Å for A = Ba, Sr (*5*, *8*, *9*)] and $YBa_2Cu_3O_{6+\delta}$ [2.88–3.00 Å (*28*)] to the corresponding alkaline earth peroxide [Ba = 2.79 Å (*18*) and Sr = 2.64 Å (*19*)]. Thus energetically the process of oxygen ion accommodation is similar in the alkaline earth-doped cuprates and the alkaline earth oxides. As energetically the overall oxidation as well as the accommodation of the oxygen ion in the doped cuprates and the alkaline earth oxides is similar; the holes in these materials must energetically be in similar states. Therefore, the thermochemical data could be interpreted to indicate that the holes, in high oxidation state cuprates, are *energetically* in peroxidelike states and upon oxidation the valence of copper remains 2+.

Structural Implications of Peroxidelike Bonds

From the thermochemical analysis, it has been suggested that energetically the holes in high oxidation cuprates are in peroxidelike states. In chemical terms, the peroxide anion has certain well-defined characteristics. For example, O_2^{2-} has a distinct spectroscopic signature. X-ray photoemission and absorption spectroscopy and Auger spectroscopic studies have claimed to have observed peroxidelike signature in $NaCuO_2$, $La_{2-x}Sr_xCuO_{4-x/2+\delta}$, and $YBa_2Cu_3O_{6+\delta}$ (*29–32*, *51*). However, there are some doubts about the validity of the interpretation of the XES and the XAS measurements [refer to, for example (*33–35*)]. As a result of this controversy spectroscopic measurements cannot yet be considered conclusive evidence for or against peroxidelike states in high oxidation cuprates.

Another unique characteristic of the peroxidelike O–O species is its well-defined bond length. In the peroxides of Ba, Sr, Ca, K, Na, Li, and Rb the O–O (peroxide) bond length is 1.50 (1) Å (*18*, *19*, *36–38*). However, even the closest O–O separation in compounds with noninteracting oxide ions (true ionic oxides, for instance) is much longer. A noninteracting O–O distance can be calculated from the ionic radius of oxygen to be 2.80 Å (*39*). In a compound like $SrTiO_3$, where the oxygen ions are in an almost ideal cubic close-packed array (with the Sr ions), the O–O distance is 2.76 Å (*40*), which is in good agreement with the value estimated from the ionic radius. Thus, if the holes that have been shown energetically to be in peroxidelike states are also *chemically* in peroxidelike states, then at least some of the O–O distances in the high oxidation state cuprates should reflect the short O–O peroxide separation. The following section examines the structural data of various high oxidation cuprates for the chemical peroxidelike signature through O–O contraction. It is important to emphasize that, unlike most of the structural observations in the literature, we are in this paper looking at changes in O–O (anion–anion) distances rather than cation–anion distances (e.g., Cu–O distances).

$NaCuO_2$ and $KCuO_2$

Figures 2 and 3 show the structure of $NaCuO_2$ and $KCuO_2$, respectively. In both structures copper is in pseudo-square planar

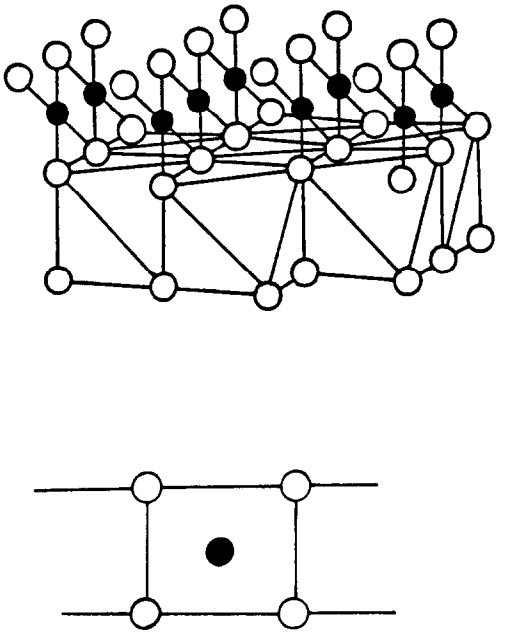

FIG. 2. The structure of $NaCuO_2$ redrawn from (*41*). The open circles represents the oxygens and the closed circles represent coppers. Na atoms are not shown but they occupy the oxygen octahedra. The bottom of the figure shows the "1-D" CuO_2 ladder.

coordination. The CuO_2 "squares" form 1-D ladders as shown in the bottom of Figs. 2 and 3. The O–O pairs forming the rungs of the ladder are much closer than the O–O pairs along the ladder. Table II lists the O–O distances of the ladder, obtained from the neutron diffraction measurements of Brese *et al.* (*41*). We argue that the short O–O distances along the rungs of the CuO_2 ladder result from holes in the peroxidelike states between the rung oxygens, causing the O–O separation to contract. The longer O–O distances along the ladder are believed to be the noninteracting oxygen separations in the structure. In $KCuO_2$ the noninteracting O–O distances range from 2.63 to 2.78 Å. These distortions are thought to be caused by the coordination requirements of the large K ion. We note that the observed short O–O separation (shorter than the noninteracting O–O distance of ~2.7 Å) in these materials attributed to the peroxide like states implies attractive interaction (bond formation). Indeed, this attractive interaction between adjacent oxygens that results in the peroxidelike state distinguishes it from the anion–anion repulsive interaction used to model anion–anion distortions seen in compounds such as $PdCl_2$ (*48*).

The difference between the average O–O separation along the rung and O–O distance along the noninteracting oxygens of the ladder is designated as the O–O peroxidelike contraction. The average O–O contraction can be calculated by assuming that every pair of holes in the peroxidelike state corresponds to a pair of O–O in the structure with the peroxide separation of 1.50 Å. Mathematically the relationship between the peroxidelike hole concentration, w, and the O–O contraction is given by

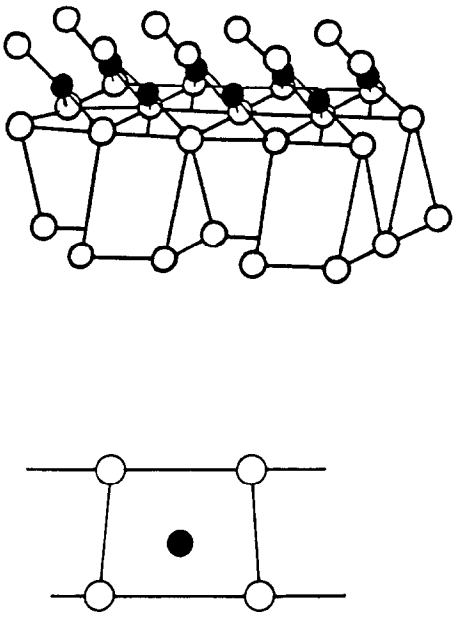

FIG. 3. The structure of $KCuO_2$ redrawn from (*41*). The open circles represents the oxygens and the closed circles represent coppers. K atoms are not shown but they occupy the oxygen triprisms. The bottom of the figure shows the "1-D" CuO_2 ladder.

TABLE II

OXYGEN DISTANCES IN THE CuO_2 LADDER AND O–O CONTRACTIONS IN $NaCuO_2$ AND $KCuO_2$

	O–O distance[a] (Å)	Contraction	
		Measured (Å)	Predicted[b] (Å)
$NaCuO_2$ (300 K)			
Along the rung	2.446		
Along the ladder	2.747	0.301	0.312
$KCuO_2$ (300 K)			
Along the rung	2.460		
Along the ladder (1)[c]	2.779	0.319	0.320
Along the ladder (2)[c]	2.634	0.174	0.284

[a] From neutron diffraction measurements of Brese *et al.* (*41*).
[b] Calculated from the "peroxide" model. See text.
[c] There are additional distortions in $KCuO_2$. See text and Fig. 5.

$$\text{O–O contraction} = \frac{[(\text{O–O})_n - (\text{O–O})_p]}{F * L} * w/2, \quad (7)$$

where $(O–O)_p$ is the O–O distance in a peroxide (1.50 Å), $(O–O)_n$ is the noninteracting oxygen distance (2.7–2.8 Å), F is the number of O–O pairs per unit cell where the peroxidelike bonds can form, and L is a geometric factor that depends on the dimensionality of the CuO_2 square layer.[1] If one assumes that all the holes in excess of the Cu^{2+} state in $NaCuO_2$ and $KCuO_2$ are in peroxidelike states, then the O–O contraction can be calculated. The last two columns of Table II list the measured and the calculated O–O contractions for $NaCuO_2$ and $KCuO_2$. The agreement between the measured contraction and the contraction calculated based on the peroxide hypothesis is very satisfactory.

[1] The dimensionality factor, L, is calculated by modeling the CuO_2 planes as isotropic, harmonically elastic sheets. L can be shown to be 1 for the 1-D ladder geometry found in $NaCuO_2$ and $KCuO_2$. For 2-D sheet geometry, in fact for a more general case of n 2-D coupled sheets, the dimensionality factor L can be shown to be equal to

$$L = \frac{e^{1/n} + 1}{e^{1/n} - 1}. \quad (8)$$

In $La_{2-x}Sr_xCuO_{4-x/2+\delta}$ the CuO_2 sheets are isolated from each other and hence n is 1 and $L = 2.16$. However, in $YBa_2Cu_3O_{6+\delta}$ two CuO_2 sheets face each other; they are separated from other such coupled sheets by the rest of the structure; and n is 2 and $L = 4.08$.

$La_{2-x}Sr_xCuO_{4-x/2+\delta}$

La_2CuO_4 (and acceptor-doped La_2CuO_4) has the K_2NiF_4 structure. The structure is composed of layers of perovskitelike oxygen octahedra separated by rocksaltlike La–O layers and can be looked upon as the first member of Ruddlesden–Popper series $LaO \cdot nLaCuO_3$ ($n = 1$) (*20*, *21*). Copper occupies the oxygen octahedral cavity of the structure. These octahedra are apically elongated, forming basal sheets of CuO_2. The intervening rocksalt La–O layers are thought to isolate the CuO_2 sheets from each other, creating a 2-D conduction geometry (*25–27*).

In the process of oxidation of $La_{2-x}Sr_xCuO_{4-x/2H\delta}$, oxygen vacancies in the CuO_2 planes are filled. Electrical conductivity measurements on single crystals demonstrate that the holes generated upon oxidation are in the CuO_2 planes (*26*, *27*). Hence, as evident from Eq. (2) the net formal charge in the CuO_2 planes remains unchanged upon oxidation but the number of (oxygen) atoms in the CuO_2 planes increases as oxygens fill vacancies in the planes. The CuO_2 planes, however, shrink (O–O distances contract) (*42*) rather than expand as expected from a simple packing argument. The average shrinkage of O–O distance upon insertion of holes in this layer is precisely what would be predicted if the holes occupied peroxidelike states with short peroxidelike O–O distances. This peroxide–like O–O contraction can be calculated from Eqs. (7) and (8). Notice that in $La_{2-x}Sr_xCuO_{4-x/2+\delta}$, unlike $NaCuO_2$, O–O shortening is along both the legs of the CuO_2 square. Figure 4 is a plot of the CuO_2 plane O–O contraction against the hole concentration obtained from the measurements of Takayama-Muromachi and Rice on $La_{2-x}Sr_xCuO_{4-x/2+\delta}$ ($x = 0.3$) (*42*).

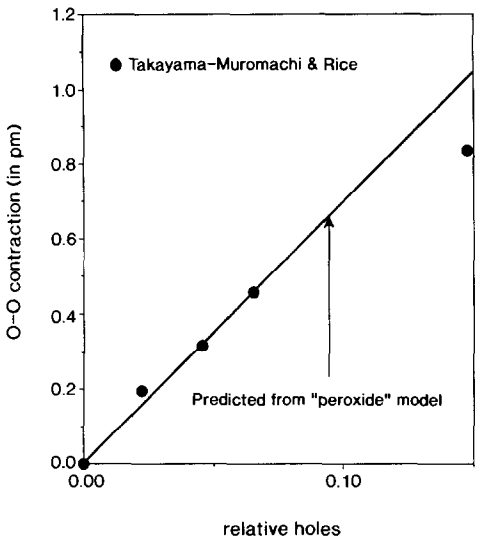

FIG. 4. The O–O contraction as a function of relative hole concentration (= $2\Delta\delta$) in $La_{2-x}Sr_xCuO_{4-x/2+\delta}$ (x = 0.3) from the measurements of Takayama-Muromachi and Rice (*42*). The solid line is predicted from the "peroxide" hypothesis. See text for details.

The solid line in Figure 4 is the predicted O–O contraction from the peroxide hypothesis [Eqs. (7) and (8)]. The measurements and the prediction are in good agreement. However, at the highest hole concentration the O–O contraction is significantly smaller than predicted. We believe that the deviation at high hole concentration is real; in fact, in $YBa_2Cu_3O_{6+\delta}$, where the hole concentration can get much larger, this effect is even more pronounced (see below).

$YBa_2Cu_3O_{6+\delta}$

$YBa_2Cu_3O_X$ crystallizes in a defect perovskite structure. Oxygens are absent from the Y planes, creating two CuO_2 sheets facing each other across the Y layer. The other Cu in the structure does not possess a full octahedral coordination of an ideal perovskite either. In the orthorhombic ($\delta > 0.4$) form of the structure all the 010 strings of oxygens are absent, forming 1-D chains of Cu–O. For $\delta < 1$, some of the oxygen along the chains is absent too, resulting in fragmentation of the Cu–O chains. At a lower δ (< 0.3), the oxygens in the chains disorder between the "chain sites" and the normally vacant 010 oxygen sites, resulting in a tetragonal unit cell.

The stoichiometric composition (n = p point) for $YBa_2Cu_3O_X$ was determined to be $YBa_2Cu_3O_6$ from high temperature electrical conductivity measurements (*15–17*). Oxidation of the stoichiometric material inserts an oxygen ion and two holes into the basal plane. Above $\delta = 0.3$, the basal plane oxygens order to form chains of Cu–O and the structure becomes orthorhombic. Also at about the same oxygen stoichiometry range as the tetragonal–orthorhombic transition there takes place an "electronic" phenomena, commonly referred to in the literature as the phenomenon of *charge transfer* (*43*). After charge transfer, at least some fraction of the newly generated holes go to the CuO_2 plane rather than the basal plane. The CuO_2 planes of $YBa_2Cu_3O_{6+\delta}$ after charge transfer are, thus, electrically comparable to CuO_2 planes of (p-type) $La_{2-x}Sr_xCuO_{4-x/2+\delta}$. Though the orthorhombic–tetragonal transition and the phenomenon of charge transfer takes place at about the same stoichiometry, there is no demonstrated causal relationship between the two phenomena.

The distance between the oxygens in the CuO_2 planes of $YBa_2Cu_3O_{6+\delta}$ shows, not unlike $La_{2-x}Sr_xCuO_{4-x/2+\delta}$, a peculiar behavior. Before the material has undergone the charge transfer transition ($\delta < 0.3$) the CuO_2 plane oxygen distance increases upon oxidation. This increase reflects the expansion of the basal plane upon incorporation of excess oxygens. However, after the material undergoes the phenomenon of charge transfer, the CuO_2 plane O–O distance *decreases* upon further oxidation. We attribute this anomalous decrease to the incorporation of the holes into peroxidelike states in the CuO_2 planes.

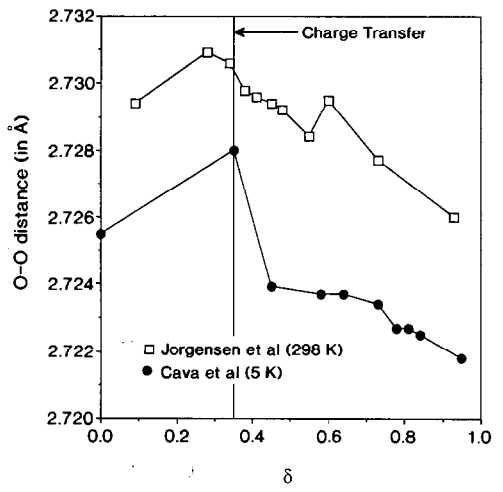

FIG. 5. The CuO_2 plane O–O distances as a function of stoichiometry, δ, in $YBa_2Cu_3O_{6+\delta}$ from the measurements of Cava *et al.* (5 K) (*28*) and Jorgensen *et al.* (298 K) (*44*).

Figure 5 shows the CuO_2 plane O–O distances as obtained from the neutron diffraction measurements of Jorgensen *et al.* (*44*) and Cava *et al.* (*28*). The two sets of measurements look similar, although they are vertically displaced. The vertical separation of the curves is presumably due to the fact that one set of measurements was performed at room temperature (Jorgensen *et al.*), whereas the other set was performed at 5 K (Cava *et al.*). In $YBa_2Cu_3O_{6+\delta}$ before charge transfer there are no holes in the CuO_2 planes, and hence it is unlikely that there is a peroxidelike interaction between the oxygens of the CuO_2 planes. Hence the CuO_2 plane distance in such a material could be taken as the noninteracting O–O distance for that stoichiometry. The noninteracting O–O distance increases with oxygen nonstoichiometry (see Fig. 5). From a linear extrapolation of this relationship the noninteracting CuO_2 plane O–O distance for any stoichiometry could be determined. The peroxidelike O–O contraction for $YBa_2Cu_3O_{6+\delta}$ can, thus, be determined. Figure 6 shows measured O–O contraction versus the oxygen stoichiometry for the two sets of neutron diffraction measurements (Cava *et al.* and Jorgensen *et al.*). The peroxidelike O–O contraction can be estimated [from Eqs. (7) and (8)] if the concentrations of the peroxidelike holes is known. The dashed line in Fig. 6 indicates the estimated O–O contraction if all the holes after the phenomenon of charge transfer ($\delta = 0.35$) go into the peroxidelike states in the CuO_2 planes. For intermediate oxygen stoichiometry ($\delta \approx 0.5$) and thus for a low peroxidelike hole concentration the agreement between the dashed line and the estimated O–O contraction is good. However, at higher oxygen content there are significant deviations. We believe that at high hole concentrations only a fraction of the holes generated after charge transfer are in peroxidelike states in the CuO_2 planes and a significant fraction of the holes reside in the chains. Modified Mont-

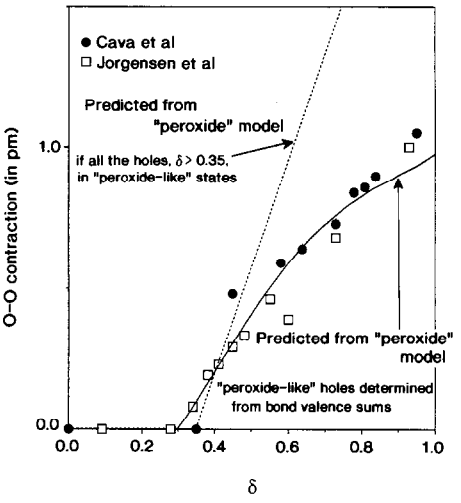

FIG. 6. The O–O contraction as a function of oxygen stoichiometry in $YBa_2Cu_3O_{6+\delta}$. The dashed line is predicted on the assumption that all the holes after $\delta > 0.35$ go into the "peroxidelike" states. The solid curve is predicted from the "peroxide" hypothesis based on the determination of the holes in the CuO_2 plane from bond valence sums. See text for details.

gomery resistivity measurements on detwinned crystals seem to support this point of view (*49*). Brown (*45*) also came to a similar conclusion from the determination of the hole distribution in $YBa_2Cu_3O_{6+\delta}$ based on bond valence sums. The method of bond valence sums is an empirical formulation that determines the charge in a bonding geometry. It takes into account only the bonds between atoms of opposite formal charges and ignores the interactions between like-charged species. Bond valence sums do not depend on the distribution of the charge in a bonding scheme, but depend only on the amount of charge in that bonding arrangement (*45*). For example, the bond valence sum around a CuO_2 bonding scheme is the same if the extra holes are on the copper, on the oxygen, or between two oxygens in peroxidelike states as long as the total number of holes in the Cu–O bonding geometry is the same. The charge around the plane Cu in $YBa_2Cu_3O_{6+\delta}$ can be determined from the method of bond valence sums and by making the additional assumption that the valence of Y and Ba remains fixed at 3+ and 2+, respectively [see Brown and Altermatt (*46*), and Brown (*45*) for details]. It is important to note that in the bond valence formulation *all* the nearest (first neighbor) cation–anion bonds have to be utilized. Hence, in determining the charge around the plane Cu not only the four close copper–plane oxygen bonds have to be counted but also the long copper–apical oxygen bond has to be considered. We assign the holes *around* (not on) the plane Cu into peroxidelike states and then estimate the O–O contraction in the CuO_2 plane [from Eqs. (7) and (8)]. The solid curve in Fig. 6 is the predicted O–O contraction from the determination of the peroxidelike hole concentration from a bond valence analysis of the structural data of Cava *et al.* (*28*). Agreement between the measured and the predicted O–O contraction is very satisfactory; strongly supporting the hypothesis that all the holes in the CuO_2 planes are in peroxidelike states.

An independent argument for the existence of peroxidelike hole states in $YBa_2Cu_3O_{6+\delta}$ can be made based on the time-dependent structural phenomena observed by Jorgensen *et al.* (*47*) on $YBa_2Cu_3O_{6.41}$. Jorgensen *et al.* prepared the sample by annealing at 520°C and quenching into liquid nitrogen. The "as prepared" sample did not exhibit superconductivity. A portion of the sample was mounted on a neutron diffraction stage held at room temperature and the structure was monitored with time. On the second portion of the sample susceptibility measurements were performed periodically. After 9000 min at room temperature the sample exhibited bulk superconductivity at 20 K. Time-dependent neutron diffraction measurements show that the increase in T_c is accompanied by a significant contraction of all three crystallographic axes [refer to Figs. 2 and 3 of (*47*)]. The average O–O distance of the adjacent oxygens of the CuO_2 plane consequently shrank too. Jorgensen *et al.* specifically looked for changes in the average occupancy of the various oxygen sites to test if the oxygen ordering was responsible for the time-dependent phenomena, but observed no significant change in the occupancies. They also saw clear evidence for charge (hole) transfer from chains to the planes; for example, they attributed the *c* axis contraction to the phenomenon of charge transfer. Similar aging phenomena were observed for a series of $YBa_2Cu_3O_{6+\delta}$ ($0.4 < \delta < 0.8$) samples by Veal *et al.* (*50*). Both Veal *et al.* and Jorgensen *et al.* propose that the aging phenomena could be a result of Cu–O chain rearrangement. It is a plausible model for the aging phenomena, at least near the oxygen stoichiometry of 6.5. However, their model is forced to invoke convoluted, if not impossible, mechanisms to explain certain related phenomena such as the contraction of O–O distances in the CuO_2 plane, re-

flected in the contraction of both *a* and *b* crystallographic axes. We believe that these observations can be very easily modeled by the peroxide hypothesis.

As argued from the thermochemical observations, energetically the holes prefer to be paired in peroxidelike bonding states; however, entropy will always favor the unpaired states. Therefore, at high temperatures, thermal disorder will excite the holes to the energetically less favorable unpaired states. It is conceivable that in the sample quenched from 520°C, most of the holes are frozen into the thermally disordered unpaired hole states. At room temperature, however, the metastable, unpaired hole states slowly revert to the more stable peroxidelike states. If the peroxidelike interactions take place in the CuO_2 planes, then with annealing (at room temperature) holes will move to the CuO_2 planes to form Peroxidelike states—transferring charge from the chains to the planes. It is also plausible that for the oxygen stoichiometry near 6.5 additional holes could be transferred from the chains to the planes by Cu–O chain reordering as suggested by Veal *et al.*, thus increasing the concentration of the peroxidelike holes in the CuO_2 plane. The average CuO_2 plane O–O separation due to these peroxidelike states is shorter, as argued earlier, and thus the average O–O distance in the CuO_2 plane will shrink with annealing. The average O–O separation as a function of the annealing time can be obtained from Jorgensen *et al.*'s neutron diffraction measurements for the oxygen stoichiometry of 6.41. The O–O separation in the "as quenched" sample is 2.7330(1) Å. The separation decreases to 2.7320(1) Å after 1500 min. The CuO_2 plane O–O shrinkage is reflected in the contraction of the *a* and the *b* axes of the cell. In the orthorhombic form of $YBa_2Cu_3O_{6+\delta}$, the Cu–O chains are along the *b* axis of the cell and hence it is possible that the *b* axis in the orthorhombic phase is more rigid. It is, thus, predominantly through the motion of the oxygen along the *a* axis (O(2)) toward the oxygen along the *b* axis (O(3)) that the peroxidelike interaction takes place. The peroxidelike contraction is, therefore, predominantly reflected in the contraction of the *a* axis of the cell, though the more rigid *b* axis of the cell would also contract slightly. This disproportionate motion of the oxygens is also reflected in the difference between the two CuO_2 plane oxygen thermal parameters. The thermal parameters for the *a* axis oxygens is approximately two times larger than that for the *b* axis oxygens (*28*, *44*).

It has, thus, been demonstrated that the structural data on these four high oxidation state cuprates can very satisfactorily be modeled by a hypothesis that assigns the holes, which thermochemically seem to be in peroxidelike states, the short peroxide O–O separation (of 1.5 Å) found in alkali and alkaline earth peroxides.

Peroxidelike Hole Pairs and Superconductivity

$NaCuO_2$ and $KCuO_2$ are insulators. There is, however, a range of oxygen stoichiometry over which $La_{2-x}Sr_xCuO_{4-x/2+\delta}$ and $YBa_2Cu_3O_{6+\delta}$ are metallic conductors. Furthermore, in the right range of stoichiometry both $La_{2-x}Sr_xCuO_{4-x/2+\delta}$ and $YBa_2Cu_3O_{6+\delta}$ superconduct. From the aging measurements of Jorgensen *et al.* (*47*) (see the previous section), one observes that the T_c increases as the CuO_2 plane O–O contracts. T_c has also been measured for samples in the two sets of neutron diffraction measurements (*28*, *44*) discussed in the last section. Figure 7 shows T_c versus the CuO_2 plane O–O contraction for the two sets of data. It suggests a linear relationship between the T_c and the O–O contraction. Since the CuO_2 plane O–O contraction is directly related to the peroxidelike hole concentration in the CuO_2 planes [as given by Eq. (7)], Fig. 7 also suggests a linear

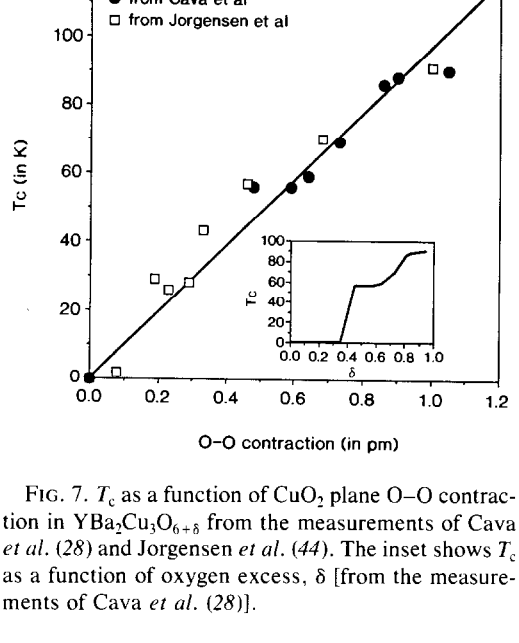

FIG. 7. T_c as a function of CuO_2 plane O–O contraction in $YBa_2Cu_3O_{6+\delta}$ from the measurements of Cava *et al.* (*28*) and Jorgensen *et al.* (*44*). The inset shows T_c as a function of oxygen excess, δ [from the measurements of Cava *et al.* (*28*)].

relationship between T_c and the peroxidelike hole concentration. This linear trend is different from the "plateau" behaviour of T_c with oxygen nonstoichiometry, δ, and hence the total hole concentration (see inset in Fig. 7). We conclude that only the holes in the CuO_2 planes, which participate in peroxidelike pair formation (and hence cause the O–O bond contraction), appear closely tied to superconductivity. Chakraverty *et al.* (*22*) and de Groot *et al.* (*23*) have proposed a Hamiltonian for a form of peroxidelike hole pair which could be responsible for charge transport in cuprate superconductors.

A purely phenomenological argument relating T_c and peroxidelike pairs can be presented as follows. A peroxidelike hole pair is composed of paired fermions and hence can be viewed as a boson. In the framework of a noninteracting (2-D) Bose–gas system, the ground state peroxidelike pair density (n_g) is related to T_c, the boson condensation temperature, by

$$n_g = \frac{w/2}{A} = \frac{2\pi m^* k T_c}{h^2}, \qquad (9)$$

where w is the peroxidelike hole concentration, A is the area of the CuO_2 plane (in a unit cell), k is Boltzmann's constant, h is Planck's constant, and m^* is the effective mass of a peroxidelike hole pair. Equation (9) predicts a linear relationship between T_c and peroxidelike hole concentration, and hence between T_c and O–O contraction, just as seen in Fig. 7. The effective mass of a peroxidelike pair in $YBa_2Cu_3O_{6+\delta}$ can, thus, be determined from Fig. 7 and is found to be about 50 m_e (where m_e is the mass of an electron). Some preliminary work on doped La_2CuO_4 suggests that the effective mass of a peroxidelike boson in that system is also about 50 m_e. A large effective mass of 50 m_e is very plausible for a species like the peroxidelike hole pair which has a large lattice distortion associated with it and hence is not very mobile. Conventional ideas about electrical conduction would argue that hole species with large effective masses could not be very mobile, yet the linear correlation between T_c and O–O contraction (see Fig. 7) suggests a strong physical significance of the peroxidelike state. One must also remember that only a fraction of the holes in these materials are in peroxidelike states and thus the conduction properties could be a composite of both peroxidelike and "normal" behavior. Clearly much work needs to be done to explore the physical implications (for example, for superconductivity) of the chemical (thermochemical and structural model presented here.

Acknowledgments

We thank J. Bularzik (of Inland Steel), J. Bringley (of Kodak), and B. Scott (of I.B.M.) for fruitful collaboration and discussions. We also thank P. Anderson, R. Bhatt, D. McClure, and S. Shyamsunder of Princeton University for valuable discussions. This work was supported by the Department of Energy (Grant DE-HGO2-89ER45394).

References

1. R. J. Cava, R. B. van Dover, B. Batlogg, and E. A. Rietman, *Phys. Rev. Lett.* **58**(4), 408 (1987).
2. E. E. Alp, G. K. Shenoy, D. G. Hinks, D. W. Capone, II, L. Soderholm, H.-B. Schuttler, J. Guo, D. E. Ellis, P. A. Montano, and M. Ramanathan, *Phys. Rev.* **35**(13), 7199 (1987).
3. D. D. Sarma and C. N. R. Rao, *J. Phys. C Solid State Phys.* **20,** L659 (1987).
4. M. W. Shafer, T. Penny, and B. L. Olson, *Phys. Rev. B* **36**(7), 4047 (1987).
5. T. Kamiyama, F. Izumi, H. Asano, H. Takagi, S. Uchida, Y. Tokura, E. Takayama-Muromachi, M. Matsuda, K. Yamada, Y. Endoh, and Y. Hidaka, *Physica C* **172,** 120 (1990).
6. J. D. Jorgensen, *Jpn. J. Appl. Phys.* **26**(3), 2017 (1987).
7. K. Sreedhar and P. Ganguly, *Phys. Rev. B* **41**(1), 371 (1990).
8. J. D. Jorgensen, H.-B. Schuttler, D. G. Hinks, D. W. Capone, II, K. Zhang, and M. B. Brodsky, *Phys. Rev. Lett.* **58**(10), 1025 (1987).
9. R. J. Cava, A. Santoro, D. W. Johnson, Jr., and W. W. Rhodes, *Phys. Rev. B* **35**(13), 6716 (1987).
10. F. A. Kroger, and H. J. Vink, *in* "Solid State Physics" (F. Seitz and D. Turnbull, Eds.), vol. 3, p. 307, Academic Press, New York (1956).
11. M. Suzuki, *Phys. Rev. B* **39**(4), 2312 (1989).
12. J. Bularzik, A. Navrotsky, J. DiCarlo, J. Bringley, B. Scott, and S. Trail, *J. Solid State Chem.* **93,** 418 (1991).
13. J. DiCarlo, J. Bularzik, and A. Navrotsky, *J. Solid State Chem.* **96,** 381 (1992).
14. M. E. Parks, A. Navrotsky, K. Mocala, E. Takayama-Muromachi, A. Jacobson, and P. K. Davies, *J. Solid State Chem.* **79,** 53 (1989); *J. Solid State Chem.* **83,** 218 (1989). [Erratum]
15. A. Mehta and D. M. Smyth, in *"Non-Stoichiometric Compounds: Surfaces, Grain Boundaries, and Structural Defects"* (J. Nowotny and W. Weppner, Eds.), p. 509, Kluwer, Dordrecht (1989).
16. D. J. L. Hong, A. Mehta, P. Peng, and D. M. Smyth, *Ceram. Trans.* **13,** 129 (1990).
17. D. J. L. Hong and D. M. Smyth, *J. Am. Ceram. Soc.* **74**(7), 1751 (1991).
18. S. C. Abrahams and J. Kalnajs, *Acta Crystallogr.* **7,** 838 (1954).
19. N. G. Vannerberg, *Ark. Kemi.,* 917 (1959).
20. D. M. Smyth, *Ceram. Superconductors* **2,** 1 (1988).
21. S. N. Ruddlesden and P. Popper, *Acta Crystallogr.* **11,** 54 (1958).
22. B. K. Chakraverty, D. Feinberg, Z. Hang, and M. Avignon, *Solid State Commun.* **64**(8), 1147 (1987).
23. R. A. de Groot, H. Gutfreund, and M. Weger, *Solid State Commun.* **63**(6), 451 (1987).
24. J. P. Coughlin, "Bulletin 542," U.S. Bureau of Mines (1954).
25. J. B. Torrance, Y. Tokura, A. I. Nazzal, A. Bezinge, T. C. Huang, and S. S. Parkin, *Phys. Rev. Lett.* **61**(9), 1127 (1988).
26. S. Kambe, K. Kitazawa, M. Naito, A. Fukuoka, I. Tanaka, and H. Kojima, *Physica C* **160,** 35 (1989).
27. S.-W. Cheong, Z. Fisk, R. S. Kwok, J. P. Remeika, J. D. Thompson, and G. Gruner, *Phys. Rev. B* **37**(10), 5916 (1988).
28. R. J. Cava, A. W. Hewat, E. A. Hewat, B. Batlogg, M. Marezio, K. M. Rabe, J. J. Krajewski, W. F. Peck, Jr., and L. W. Rupp, Jr., *Physica C* **165,** 419 (1990).
29. C. N. R. Rao, P. Ganguly, M. S. Hegde, and D. D. Sarma, *J. Am. Chem. Soc.* **109,** 6893 (1987).
30. D. D. Sarma and C. N. R. Rao, *J. Phys. C Solid State Phys.* **20,** L659 (1987).
31. J. C. Fuggle, P. J. W. Weijs, R. Scoorl, G. A. Sawatzky, J. Fink, N. Nucker, P. J. Durham, and W. M. Temmerman, *Phys. Rev. B* **37**(1), 123 (1988).
32. Also refer to the section on high energy spectroscopy in the "Proceedings of the International Conference on High Temperature Superconductors: Materials and Mechanism of Superconductivity, Interlaken, Switzerland (28 Feb.–4 Mar. 1988)," as reproduced in *Physica C* **153–155,** 111 (1988).
33. B. H. Brandow, *J. Solid State Chem.* **88,** 28 (1990).
34. R. S. List, A. J. Arko, Z. Fisk, S.-W. Cheong, S. D. Conradson, J. D. Thompson, C. B. Pierce, D. E. Peterson, R. J. Bartlett, N. D. Shinn, J. E. Schirber, B. W. Veal, A. P. Paulikas, and J. C. Campuzano, *Phys. Rev. B* **38**(16), 11966 (1988).
35. R. S. List, A. J. Arko, R. J. Bartlett, C. G. Olson, A-B. Yang, R. Liu, C. Gu, B. W. Veal, Y. Chang, P. Z. Jiang, K. Vandervoort, A. P. Paulikas, and J. C. Campuzano, *Physica C* **159,** 439 (1989).
36. H. Foppl, *Z. Anorg. Chem.* **291,** 12 (1957).
37. H. Foppl, *Angew. Chem.* **66,** 335 (1954).
38. R. L. Tallman, J. L. Margrave, and S. W. Bailey, *J. Am. Chem. Soc.* **79,** 2979 (1957).
39. R. D. Shannon and C. T. Prewitt, *Acta Crystallogr. B* **25,** 925 (1969).
40. H. Swanson and Fuyat, *Natl. Bur. Stand. (U.S.)* **539,** 344 (1953).
41. N. E. Brese, M. O'Keeffe, R. B. von Dreele, and V. G. Young, Jr., *J. Solid State Chem.* **83,** 1 (1989).
42. E. Takayama-Muromachi and D. E. Rice, *Physica C* **177,** 195 (1991).

43. R. J. Cava, B. Batlogg, K. M. Rabe, E. A. Rietman, P. K. Gallagher, and L. W. Rupp, Jr., *Physica C* **156,** 523 (1988).
44. J. D. Jorgensen, B. W. Veal, A. P. Paulikas, L. J. Nowicki, G. W. Crabtree, H. Claus, and W. K. Kwok, *Phys. Rev. B* **41**(4), 1863 (1990).
45. I. D. Brown, *J. Solid State Chem.* **82,** 122 (1989).
46. I. D. Brown and D. Altermatt, *Acta Crystallogr. B* **41,** 244 (1985).
47. J. D. Jorgensen, S. Pei, P. Lightfoot, H. Shi, A. P. Paulikas, and B. W. Veal, *Physica C* **167,** 571 (1990).
48. J. K. Burdett and D. C. Caneva, *Inorg. Chem.* **24,** 3866 (1985).
49. T. A. Friedmann, M. W. Rabin, J. Giapintzakis, J. P. Rice, and D. M. Ginsberg, *Phys. Rev.* **42**(10), 6217 (1990).
50. B. W. Veal, A. P. Paulikas, H. You, H. Shi, Y. Fang, and J. W. Downey, *Phys. Rev.* **42**(10), 6305 (1990).
51. C. N. R. Rao, *J. Solid State Chem.* **74,** 147 (1988).